

<https://helda.helsinki.fi>

---

## Retinal origins of the temperature-effect on absolute visual sensitivity in frogs

Aho, A.-C.

Blackwell  
1993

---

Journal of Physiology. 1993. 463: 501-521

---

<http://hdl.handle.net/1975/963>

---

*Downloaded from Helda, University of Helsinki institutional repository.*

*This is an electronic reprint of the original article.*

*This reprint may differ from the original in pagination and typographic detail.*

*Please cite the original version.*

## RETINAL ORIGINS OF THE TEMPERATURE EFFECT ON ABSOLUTE VISUAL SENSITIVITY IN FROGS

By ANN-CHRISTINE AHO\*, KRISTIAN DONNER AND TOM REUTER

From the Department of Zoology, University of Helsinki, SF-00100 Helsinki, Finland

(Received 19 February 1992)

### SUMMARY

1. The absolute sensitivity of vision was studied as a function of temperature in two species of frog (*Rana temporaria*, 9–21 °C, and *Rana pipiens*, 13–28 °C).

2. Log behavioural threshold (measured as the lowest light intensity by which frogs trying to escape from a dark box were able to direct their jumping) rose near-linearly with warming with a regression coefficient of  $1.26 \pm 0.03$  log units per 10 °C ( $Q_{10} = 18$ ). Threshold retinal illumination corresponded to 0.011 photoisomerizations per rod per second ( $\text{Rh}^* \text{s}^{-1}$ ) at 16.5 °C.

3. The effect of dim backgrounds on jumping thresholds suggested 'dark lights' of 0.011  $\text{Rh}^* \text{s}^{-1}$  at 16.5 °C and 0.080  $\text{Rh}^* \text{s}^{-1}$  at 23.5 °C, corresponding to  $Q_{10} = 17$ .

4. Response thresholds of retinal ganglion cells were extracellularly recorded in the isolated eyecup of *R. temporaria*. The thresholds of the most sensitive cells when stimulated with large-field steps of light were similar to the behavioural threshold and changed with temperature in a similar manner.

5. The decrease in ganglion cell 'step' sensitivity with warming consisted of a decrease in summation time (by a factor of 2–3 between 10 and 20 °C) and an increase in the threshold number of photoisomerizations (a decrease in 'flash' sensitivity, by a factor of 2–5 over the same interval). No effect of temperature changes on spatial summation was found.

6. Frequency-of-response functions of ganglion cells indicated an 11-fold increase in noise-equivalent dark light between 10 and 20 °C (mean values in four cells 0.009 vs. 0.10  $\text{Rh}^* \text{s}^{-1}$ ).

7. The temperature dependence of ganglion cell flash sensitivity could be strongly decreased with dim background illumination.

8. It is concluded that the desensitization of dark-adapted vision with rising temperature is a retinal effect composed of shortened summation time and lowered flash sensitivity (increased numbers of photons required for a threshold response) in ganglion cells. The desensitization bears no simple relation to the apparent retinal noise increase.

\*Authors names appear in alphabetical order.

## INTRODUCTION

Light detection requires that a stimulus-induced change in the state of excitation of the visual system ('signal') be distinguished from random variability in the absence of a stimulus ('noise'). This variability can either be the neural response to quantal fluctuations in the numbers of background photons ('extrinsic' noise) or an inherent property of the system itself ('intrinsic' noise). Total noise sets a theoretical limit to the system's ability to detect light stimuli (de Vries, 1943; Rose, 1948; Barlow, 1956, 1957).

Noise associated with the molecular events of transduction and transmission is *a priori* likely to increase with temperature, and this is an experimentally recorded fact at least for membrane voltage fluctuations in dogfish bipolar cells (Ashmore & Falk, 1977) and dark current fluctuations in toad rods (Baylor, Matthews & Yau, 1980). We therefore use temperature changes in an attempt to manipulate noise in naturally behaving frogs. Our primary objective has been to clarify the role of thermal retinal noise in limiting absolute visual sensitivity. Noise-limited sensitivity should drop when temperature rises.

Warming will, however, also accelerate light responses (Baylor, Matthews & Yau, 1983; Lamb, 1984; Donner, Hemilä & Koskelainen, 1988), implying that the temporal integration of photon signals decreases (and temporal resolution improves). This is another factor likely to desensitize natural vision, which is usually concerned with objects of relative permanence in time. We further had to consider the possibility that *spatial* summation could change with temperature, which would also affect sensitivity.

We have previously reported that visual sensitivity in amphibians does indeed fall with rising temperature, a correlation which can even be qualitatively generalized to human vision at 37 °C (Aho, Donner, Hydén, Larsen & Reuter, 1988). Here we make a quantitative determination of the temperature dependence of sensitivity in two closely related species of frog. The effect is strong and consistent, a sensitivity drop by more than one order of magnitude for a temperature rise from 10 to 20 °C. The sensitivity of retinal ganglion cells to stimuli equivalent to those used in the behavioural experiment (large fields of long duration) is shown to depend on temperature in a very similar manner, allowing the conclusion that the effect is of retinal origin. Analysing the effect in ganglion cells, we find that it is composed of two changes in roughly equal proportions: a decrease in temporal summation and an increase in the number of photo-isomerizations required for a threshold response (a decrease in 'flash' sensitivity). The latter change was strongly decreased if a sufficient amount of temperature-independent background (photon) noise was applied. We therefore think that the thermal drop in flash sensitivity is really noise related, although it is larger than would be necessary just to maintain a constant signal-noise ratio of threshold responses, given the temperature dependence of retinal noise.

## METHODS

*Animals*

All electrophysiology and part of the behavioural experiments were done on *Rana temporaria* caught in the wild in October in southern Finland and kept in basins at 5 °C without feeding. In

February 1990, the frogs to be used in behavioural experiments (mean body length  $67 \pm 5$  mm, 24 frogs) were transferred to 15 °C, and after 1–2 weeks acclimation to that temperature, sessions were begun. Harri (1973) has measured oxygen consumption and blood glucose in frogs transferred from 5 to 25 °C, or vice versa, concluding that acclimation is complete within 1 week both for winter and summer frogs. *R. temporaria* were tested at 12, 13–14, 15–16, 17–18 and 21 °C. A separate series of behavioural sessions at 21 °C was conducted in August with freshly collected summer frogs (mean body length  $77 \pm 6$  mm, 11 frogs); the purpose was to check how strongly season or acclimation conditions could affect the results. Differences were slight from the viewpoint of the present work.

In order to extend the testable temperature range upwards to temperatures which would be unnatural for Finnish *R. temporaria*, another series of experiments was carried out with *R. pipiens* (KONS Scientific, Co., Inc., Germantown, WI, USA; mean body length  $72 \pm 4$  mm). Twenty-four frogs were kept in room temperature (21–22 °C) and tested at 22–23 °C in January 1990. Then, after 2 weeks acclimation to 15 °C, they were tested at 13–14 °C. Twelve of the frogs were returned to room temperature for 3 weeks and tested at 25–26 °C and, 1 month later, at 27–28 °C. Another batch of sixteen *R. pipiens* was used in the autumn of 1991 for experiments with background illumination at 16–17 and 23–24 °C (Fig. 4).

The frogs used in most of the experiments were force-fed with food tablets, mealworms or meat with added vitamins, once a week when kept at 15 °C and twice a week when kept at room temperature. The 1991 *R. pipiens* were allowed to eat mealworms freely three times a week at 16–17 °C. When experiments at high temperature (23–24 °C) were conducted they were fed after each session.

The animals were kept in rooms receiving dim daylight through the windows, and thus experienced a natural light–dark cycle, varying from 6.00 h–18.00 h in January to 18.00 h–6.00 h in June (when, in fact, it never gets quite dark in Helsinki). They were never exposed to strong light. Before each session, they adapted in complete darkness for at least 2 h at the temperature of the session. The sessions lasted for 1 h.

#### *The behavioural experiment*

*General principle.* The experiment makes use of the phototactic jumping of frogs placed in a dark box (Aho, Donner, Hydén, Reuter & Orlov, 1987). Left in darkness, the frog will interpret an illuminated area as a hole through which it can escape, and will preferentially jump in that direction (cf. Muntz, 1962). By recording the proportion of light-directed jumps out of total jumps, it is possible to determine the lowest illumination where jumping still retains a criterion degree of orientation.

*Test chamber.* The frog sits in a black plastic bucket of 30 cm height, 20 cm bottom diameter and 26 cm opening diameter. Nineteen centimetres above the bottom, four pairs of infrared emitter–detector pairs are placed symmetrically in the walls of the bucket so as to form the corners of a square, subdividing the chamber into four equal sectors (see Fig. 1A). This detection plane lies too high for a frog of 7 cm body length to reach by fully stretching its legs and body, while, on the other hand, most jumps exceed 19 cm in height (as found by observing the frogs in light). Thus, each emitter–detector pair will record jumps, and jumps only, into one sector. In one of the sectors, there is a lit circular window in the ceiling (see below). Jumps into this sector are recorded on one pulse counter, while jumps into the three dark sectors are pooled on another counter. Four identical test chambers are placed in square-like fashion, their 'lit' sectors adjacent to each other and the light source perpendicularly above the centre of the square (Fig. 1B). Thus, four frogs could in principle be tested in one session. Yet, more than half of the material was collected with only one or two buckets in use in order to minimize possible 'co-operativity' artifacts from frogs being guided by the sound of neighbours. (Although a potential source of error, we found no evidence for this.)

In a previous study (Aho *et al.* 1987), we used square-shaped test chambers. The advantage of a circular enclosure is that the frog cannot hide in a corner. The bottom was kept moist by a thin sheet of foam-rubber soaked in water. It was found that even a shallow layer of water will decrease the willingness to jump and if there was more than 1 cm of water, the frog often preferred to lie flat rather than jump.

*Temperature control.* The test chambers were placed in a larger basin and temperature was regulated by surrounding them with circulating water and/or ice. At extreme temperatures, the whole room where the experiments were conducted was warmed or cooled to decrease the gradient between the test chambers and the surroundings. These arrangements allowed

temperature to be held within  $\pm 0.5$  °C around the chosen value. Temperature was monitored by thermistors in the chambers.

The body temperature of a frog could, depending on activity, deviate somewhat from the ambient temperature. In *R. pipiens* 'manually prodded to continuous activity' so as to be 'near fatigue after 5 minutes', Putnam & Bennett (1981) found an average increase of 1.2 °C in cloacal temperature regardless of initial body temperature. This gives an upper limit for a possible deviation, as body temperature and ambient temperature were initially equal (in the range 9–32.5 °C). At the lower temperatures in our experiments (12–18 °C), the average jumping rate ranged from 1 per 30 min to 1 per 3 min (see below) and can hardly have raised body temperature very much. At the highest temperatures, though, some frogs jumped several times per minute. Then warming relative to the environment may even have approached the value found by Putnam & Bennett (1981). The consequence would be a somewhat exaggerated apparent temperature dependence of behavioural sensitivity in the highest range. (A correction would maximally entail a 1.2 °C rightwards shift of the data points for the highest temperatures in Fig. 3.)

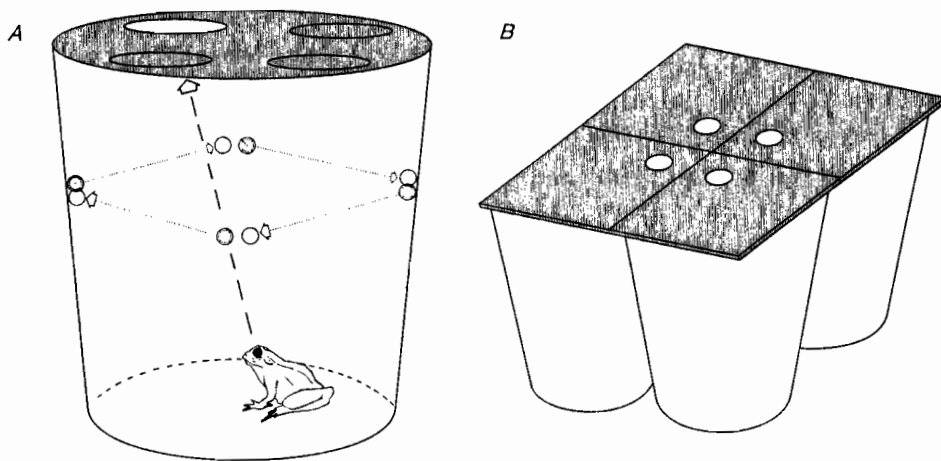


Fig. 1. The jumping chamber. A, cross section. B, general view of the group of four chambers. See text for further explanation.

*Stimulus.* The ceiling common to all four test chambers was formed by three sheets: (1) an antireflex frameglass, (2) a black cardboard sheet with a circular hole (9 cm diameter) in the centre of one of the sectors of each chamber, and (3) on top, an acryl diffuser. The light came from a 15 W halogen lamp connected to a stabilized current source (run at 1.5 A, Kikusui PAB 32-3) and enclosed in a light-tight, ventilated black box. The light passed through a light-tight filter holder where a 525 nm interference filter and any desired number of calibrated neutral density filters were inserted. Care was taken to place the filters at small angles to each other to avoid back reflection. The stimulus light passed out of the filter holder through a small hole (4 cm diameter) covered by a plastic diffuser. The perpendicular distance from this outlet to the roof of the test chambers was 1 m.

In the increment threshold experiments, the black cardboard sheet with windows was replaced by sheets of gelatin filters of desired optical density with corresponding windows. Window/background contrast was controlled by varying the density of the filter sheet.

*Rates of photoisomerizations in retinal rods.* Calibration was done as described by Aho *et al.* (1987). The light intensity (without neutral density filters) at the level of the eyes of a sitting frog (4 cm above the bottom of the chamber) was measured with a calibrated Airam UVM-8 radiometer (Kara Tekniikka Oy, Helsinki). Retinal rates of photoisomerizations from the 9 cm diameter window 26 cm above the frog's eye were calculated using the following parameters:

(1) *R. temporaria*. Red rods had average outer segment length  $43 \mu\text{m}$  and density  $15700 \text{mm}^{-2}$  retina (Henilä & Reuter, 1981). The area of the entrance pupil was  $10.0 \text{mm}^2$  (determined from face-on photographs), total corneal reflection 9% and posterior focal length  $4.48 \text{mm}$  (see du Pont & de Groot, 1974; Aho *et al.* 1987). The retinal image of the window then covers  $1.86 \text{mm}^2$  or 29200 rods. Thirty-two per cent of 525 nm quanta incident on the retina are estimated to produce isomerizations in red rods (see Reuter, Donner & Copenhagen, 1986; Copenhagen, Donner & Reuter, 1987). Possible light absorption by the ocular media was considered negligible (see Govardovskii & Zueva, 1974).

(2) *R. pipiens*. Red rods had average length  $53 \mu\text{m}$  and thickness  $7.3 \mu\text{m}$ . The total rod count per  $\text{mm}^2$  retina was 18500. Assuming that 14% are green rods (Liebman & Entine, 1968), the density of red rods is  $15900 \text{mm}^{-2}$ , not significantly different from that of *R. temporaria*. The area of the entrance pupil was  $10.2 \text{mm}^2$  and the posterior focal length  $4.98 \text{mm}$ . The retinal image of the window then covers  $2.29 \text{mm}^2$  or 36400 rods. Assuming that the retina has optical density 0.41 at 525 nm (Fig. 11 in Matthews, Hubbard, Brown & Wald, 1963) and a quantum efficiency for isomerization of 0.66, 40% of 525 nm quanta incident on the retina are estimated to produce isomerizations in red rods.

The possibility that temperature could directly affect the amount of light entering the eye by changing dark-adapted pupil size was checked by photographing *R. pipiens* in darkness (with a flashlight) at each temperature. No significant changes in pupil size were found.

#### *Analysis of jumping performance*

In each experimental condition (i.e. combination of temperature and light intensity) at least twelve frogs were tested in 1 h sessions, except for some of the lowest and very obviously subthreshold intensities, where fewer sessions were sometimes considered sufficient. On the other hand, in some conditions critical to the interpolation of threshold, extra sessions (up to a total of 24) were conducted. Denoting the number of jumps into the lit sector by  $S$  ('signal') and the summed number of jumps into the three dark sectors by  $N$  ('non-oriented'), the ratio  $S/(S+N)$  was calculated for each 1 h session with one frog.

Experimental variability arises both from individual differences in visual sensitivity between frogs and from random variation in the numbers of jumps in single sessions. Therefore, it is not possible to define a 'best' measure of the degree of orientation averaged across sessions on purely statistical grounds. At the one extreme, a mean of single-session ratios  $S/(S+N)$  would receive identical contributions, for example, from sessions with  $S=1$  and  $N=0$  and from sessions with  $S=50$  and  $N=0$ , although the latter result is much more significant. At the other extreme, a ratio of sums ( $\Sigma S/\Sigma(S+N)$ ), pooling jump counts across all sessions under one experimental condition) is liable to be dominated by a few eagerly jumping individuals. As a compromise, we calculated (for each experimental condition) a *weighted* mean of the ratios  $S/(S+N)$  from the single sessions, using the weighting factor  $\sqrt{(S+N)}$  (which reflects how the statistical accuracy of a session estimate improves with the number of jumps). The 'orientation index'  $\Omega$  thus obtained is our quantitative measure of performance under each condition:

$$\Omega = \frac{\Sigma[\sqrt{(S+N)} \times S/(S+N)]}{\Sigma\sqrt{(S+N)}} = \frac{\Sigma[S/\sqrt{(S+N)}]}{\Sigma\sqrt{(S+N)}}. \quad (1)$$

In practice, the total number of jumps of one frog in one session varied from 0 to over 500 (in an extreme case), but was typically around 10. There was a systematic dependence of general jumping activity on both light and temperature. In the sessions with the lowest light intensity at each temperature over the range  $12\text{--}18^\circ\text{C}$ , the total number of jumps per *R. temporaria* averaged  $2.2 \text{h}^{-1}$ , while for the highest-intensity sessions at the same temperatures the average was  $21 \text{h}^{-1}$ . In this temperature range there was, on the other hand, little dependence of jumping activity on temperature, but at  $21^\circ\text{C}$ , a few individuals became 'hyperactive', and the jump count (averaged across all intensities) at that temperature was  $60 \text{h}^{-1}$ . To avoid giving hyperactive frogs excessive weight, the weighting factor  $\sqrt{(S+N)}$  was not allowed to grow indefinitely: if either  $S$  or  $N$  (or both) in one session was  $>100$ ,  $\sqrt{(S+N)}$  was calculated from  $S$  and  $N$  values both scaled down by a factor that would reduce the larger of the numbers to 100. Thus, the weights of single sessions could vary from 0 (when no jumping occurred) to, in principle, a maximum of 14 ( $=\sqrt{(100+100)}$ ).

This compression of the weighting factor had to be applied only to six sessions with *R. temporaria* (3 of the 36 sessions at 21 °C in Fig. 2A and 3 of the 141 background sessions in Fig. 4A).

Since 'signal' jumps were those directed into one of four symmetrical sectors, completely random jumping would yield  $\Omega = 0.25$ . We arbitrarily chose to regard  $\Omega = 0.5$  as visual threshold, whereby signal jumps were twice as frequent as they would be by pure chance. The precise choice of threshold criterion is not critical, because in a certain range of light intensities orientation improved fairly sharply with rising intensity (see Fig. 2). A rough idea of the statistical significance of our threshold criterion can be gained by observing that every  $\Omega$  value used to interpolate threshold was based on a total jump count  $> 60$ . With  $(S + N) = 60$  and  $\Omega = 0.5$ ,  $S$  and  $N$  will both be 30, while random jumping would give  $S = 15$  and  $N = 45$ . By a  $\chi^2$  test, the two distributions differ at the  $P < 0.01$  level.

#### *Extracellular recording from single ganglion cells*

Action potentials were recorded from single ganglion cells in the *R. temporaria* eyecup preparation by conventional extracellular techniques (see e.g. Copenhagen *et al.* 1987). Before the experiments, the frogs were kept overnight in a dark room where they gradually warmed from 4 to 15 °C. The light source was a 15 W microscope lamp run by a stabilized current source at 2.3 A (Coutant LA 400.2). Flashes lasting 67 ms, or 4 or 8 s square-waves ('steps') of light were delivered by an electronic shutter (Compur). Only ganglion cells with an 'on' response component were used. Stimulus intervals were 45 or 60 s at low temperatures but 30 s at 20 °C, thought sufficient to avoid desensitization of the ganglion cell. Most experiments were recorded on tape to allow analysis of maintained activity and unambiguous identification of responses. Light calibration and the calculation of photoisomerization rates in red rods were as described by Reuter *et al.* (1986) and Copenhagen *et al.* (1987).

Temperature was controlled by gravity-driven water flow around the specimen chamber and monitored by a calibrated thermocouple in the Ringer bath surrounding the specimen holder. Changes were achieved by switching the water flow between basins at different temperatures. Temperature changes were fairly slow (*ca* 1 °C min<sup>-1</sup>) and thresholds were determined only when a steady state had been reached.

**Threshold.** Frog ganglion cells usually have a very low level of maintained discharge (one or a few spikes min<sup>-1</sup>). They have a distinct spike threshold, so in contrast to mammalian ganglion cells, the occurrence even of one spike soon after a stimulus is (usually) a statistically very significant response. It is therefore reasonable to take threshold simply as the stimulus intensity which on 50 % of the trials is followed by one or several spikes within a predefined time window (here 2 s for 'flash' thresholds). One threshold determination was normally based on about twenty stimulus presentations, whereby the accuracy is *ca*  $\pm 0.05$  log units.

**Parameters derived from threshold recordings.** Four characteristics of the ganglion cell were determined at each temperature: (1) the number of photoisomerizations within the ganglion cell's receptive field needed to produce a response on half the trials,  $M_t$ ; (2) the summation area,  $A_s$ ; (3) the summation or integration time,  $t_i$ ; and (4) the retinal illumination the onset of which produces a response in the ganglion cell on half the trials,  $I_t$  (in units of photoisomerizations per square millimetre retina per second or photoisomerizations per rod per second (Rh\* s<sup>-1</sup>)).  $M_t$  is obtained directly as the threshold to a stimulus much smaller than  $A_s$  and of duration shorter than  $t_i$ .  $A_s$  is obtained from the ratio of thresholds to two test spots, one much smaller and one larger than  $A_s$ . Often, a more useful measure of spatial summation is the number of rods ( $R$ ) within  $A_s$ , obtained by multiplying  $A_s$  by rod density.  $t_i$  is obtained from the ratio of thresholds to a brief (duration  $\ll t_i$ ) and a long pulse of light, respectively (i.e. 'flash' and 'step' thresholds).  $I_t$  corresponds to the behaviourally measured visual threshold and is related to the other parameters by

$$I_t = M_t / A_s t_i. \quad (2)$$

These parameters and the underlying assumptions are discussed in more detail by Donner (1987) and Copenhagen *et al.* (1987).

The full protocol with four threshold determinations in each condition over one cycle of temperature change (low-high-low) required that the recording and the sensitivity of the ganglion cell remained stable for at least 4 h. This is an exacting demand, and in some of the cells for which results are presented a shorter protocol was used, taking advantage of the relation expressed in eqn (2).

*Frequency-of-response functions.* To estimate retinal noise interfering with light detection, we recorded frequency-of-response functions from retinal ganglion cells. This implies determining the proportions of trials on which the cells respond to repeated presentations of flashes of a few fixed nominal intensities. The amount of variability (noise) underlying the responses can be estimated from the shape (shallowness) of the functions (see Barlow, 1977; Copenhagen *et al.* 1987; Aho *et al.* 1987; Donner, 1992).

The assumption is that a frog ganglion cell produces one or more spikes if and only if the excitation summed across its receptive field over a certain summation time ( $t_1$ ) exceeds a fixed threshold. In a perfectly noise-free retina, this would depend only on the number of photon excitations (isomerizations) received. Even then, response variability would be apparent due to quantal fluctuations of the stimulating light itself. A flash set to produce on average  $M$  photon excitations will on individual trials produce varying numbers  $m$  following Poisson statistics. If the cell's spike threshold is  $C$  quantal excitations, the relative frequency with which it would respond to the flash in a long series of trials is given by the Poisson probability

$$P(m \geq C) = \sum_{k=C}^{\infty} M^k e^{-M} / k!. \quad (3)$$

This describes the performance of an ideal, noise-free ganglion cell (photon detector). The effect of intrinsic noise in the retina is to increase the variability of responding to the flash as compared with eqn (3). It is convenient to formally *quantify* the noise that affects light detection by means of a 'noise-equivalent dark light', i.e. as a background light which by its statistical fluctuations would degrade the performance of an ideal detector to the level attained by the real cell (Barlow, 1956, 1977; Donner, 1992). Assume that on average  $X$  photon-like events occur in the receptive field within  $t_1$ . When repeatedly presented with a flash that produces an average of  $M$  photon excitations within the receptive field, the average number of excitations actually counted by the ganglion cell within  $t_1$  will be  $M + X$ . Numbers received on individual trials ( $m + x$ ) are Poisson-distributed around the mean  $M + X$ . The probability of exceeding the criterion  $C$  now becomes

$$P(m + x \geq C) = \sum_{k=C}^{\infty} (M + X)^k e^{-(M + X)} / k!. \quad (4)$$

$P$  is a function of  $M$  with two parameters ( $C$ ,  $X$ ).  $C$  defines the position of the frequency-of-response curve on the abscissa, while its steepness depends on both  $C$  and  $X$ . By means of an iterative program computing the (binomial) probability of the entire data set for any chosen values of  $C$  and  $X$ , we determined the  $X$  value for which the experimental data attained a *maximum* probability under the hypothesis embodied in eqn (4). This is the maximum-likelihood fit. The prerequisite for a unique solution in our case was that  $C$  (the position of the curve on the intensity scale) was restricted by a reliable calibration of the mean numbers of photoisomerizations  $M$  produced by a given nominal flash intensity.

Since  $X$  is the *number* of photon-like events seemingly pooled with the flash (i.e. occurring within the summation area within one summation time around the flash), the *noise-equivalent dark light* (in units of  $\text{Rh}^* \text{s}^{-1}$ ) is

$$I_x = X / R t_1. \quad (5)$$

It should still be emphasized that expressing detection-limiting noise in terms of quantal fluctuations from a noise-equivalent dark light ( $I_x$ ) is *a priori* only a convenient formalism and not necessarily committed to the idea that the noise is really due to thermal isomerizations in rods.

## RESULTS

### *Behavioural thresholds in darkness*

The orientation indices,  $\Omega$ , obtained in the jumping sessions in darkness are shown in Fig. 2 as functions of the corneal illumination from the lit window. Each symbol type corresponds to results obtained at one temperature; Fig. 2A shows data for *R. temporaria* and B for *R. pipiens*. The most complete set of data at any



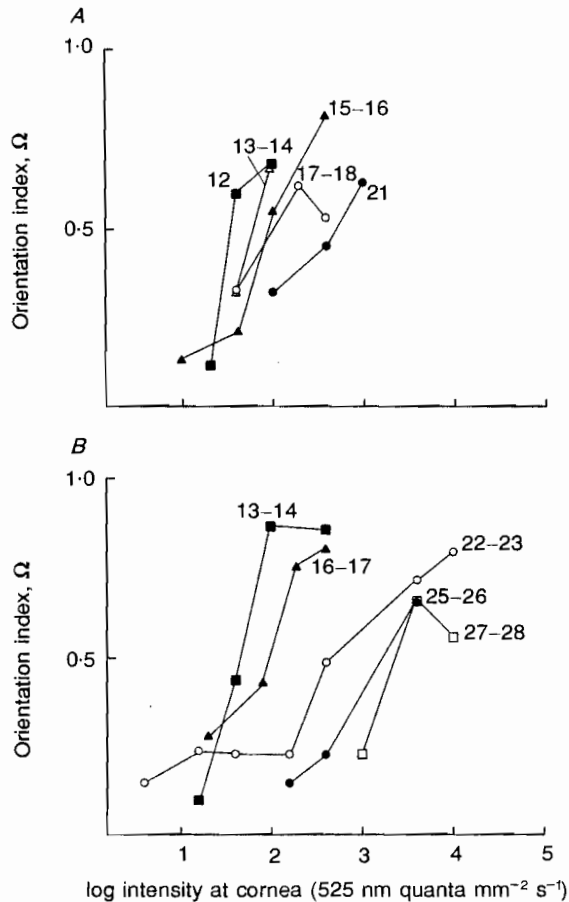


Fig. 2. The degree of orientation of phototactic jumping as a function of intensity of the lit window. The ordinate gives the orientation index,  $\Omega$ , as defined in the Methods. The abscissa is log window intensity at the cornea ( $525 \text{ nm quanta mm}^{-2} \text{ s}^{-1}$ ). Each symbol type refers to data obtained at one temperature (as indicated in the figure in  $^{\circ}\text{C}$ ). A, data from *Rana temporaria*. B, data from *Rana pipiens*. The horizontal dotted line indicates the threshold level ( $\Omega = 0.5$ ).

single temperature is that collected for *R. pipiens* at  $22\text{--}23^{\circ}\text{C}$  ( $\circ$  in B), which comprises seven different light intensities. From this set it is evident that orientation remains essentially random ( $\Omega \approx 0.25$ ) at low intensities but starts improving fairly steeply in a certain intensity range. Such a distinct threshold range is a common feature of all the sets of data; therefore we usually determined only one 'random-orientation' point in the low-intensity region. On the other hand, once there was sufficient light for reliable detection, increasing the intensity further did not necessarily improve orientation. At higher intensities,  $\Omega$  appears to be limited by behavioural factors rather than by the detectability of the light. (See  $17\text{--}18^{\circ}\text{C}$  in Fig. 2A and  $27\text{--}28^{\circ}\text{C}$  in Fig. 2B.) The secondary drop in  $\Omega$  was connected with relatively strong increases in the numbers of non-oriented jumps, suggesting increased general excitability at the highest light intensities.

Our threshold criterion  $\Omega = 0.5$  is indicated by the horizontal dotted line in Fig. 2. The threshold intensities at the different temperatures are read at the points of intersection of this line with those connecting data points. In Fig. 3, the reciprocals of these thresholds ( $1/\text{threshold} = \text{sensitivity}$ ) are plotted on a logarithmic scale against the mean temperature of the respective series of sessions.

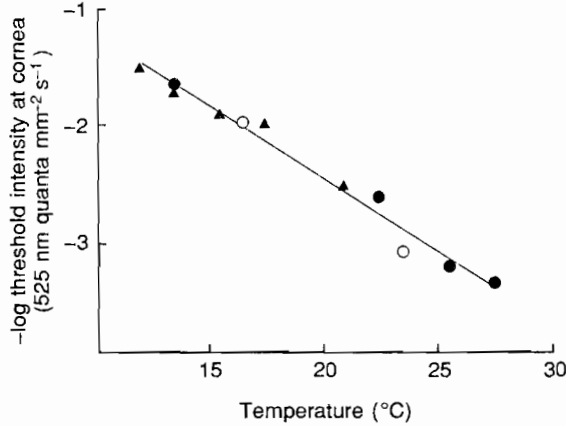


Fig. 3. Dark-adapted visual sensitivity ( $\log 1/\text{threshold}$ ) as a function of temperature. The data points give the intensities at which the curves in Fig. 2 intersect with the dotted line at  $\Omega = 0.5$ . Ordinate,  $\log$  reciprocal threshold intensity. Abscissa, temperature ( $^{\circ}\text{C}$ ).  $\blacktriangle$  marks thresholds of *Rana temporaria*, circles mark thresholds of *Rana pipiens*.  $\bullet$ , winter–spring 1990.  $\circ$ , second batch of *R. pipiens*, autumn 1991 (the original orientation function underlying the threshold at  $23.5^{\circ}\text{C}$  is shown in Fig. 4 but not included in Fig. 2 to avoid clutter). The regression line has slope  $-1.26 \pm 0.03$  log units per  $10^{\circ}\text{C}$ .

The temperature dependence of sensitivity was similar in *R. temporaria* and *R. pipiens*. Log sensitivity fell approximately linearly with temperature. A regression line fitted to the pooled data over the whole temperature range has slope  $-1.26 \pm 0.03$  log units per  $10^{\circ}\text{C}$  corresponding to an 18-fold drop in sensitivity per  $10^{\circ}\text{C}$  ( $Q_{10} = 18$ ). In the following we attempt to analyse the mechanisms underlying this regular and remarkably strong thermal desensitization.

#### Behavioural dark light

We hypothesized that the desensitization was partly due to an increase in the intrinsic noise of the visual system. Intrinsic noise cannot be directly derived from jumping performance. However, it is possible to measure an *illumination-equivalent dark light* by determining the dimmest background light that affects jumping orientation (Fechner, 1860; Aguilar & Stiles, 1954). In both frog and man, this closely corresponds to the noise-equivalent dark light described in the Methods (eqns (4) and (5); see Barlow, 1977; Aho *et al.* 1987; Donner, 1992).

The general effect of backgrounds on jumping thresholds was first characterized, and the dark light measured, in a series of sessions at  $15\text{--}16^{\circ}\text{C}$  with *R. temporaria*. Then the temperature dependence of the dark light was measured in shorter series of sessions with *R. pipiens* at two temperatures ( $16\text{--}17$  and  $23\text{--}24^{\circ}\text{C}$ ). For the background experiments, the black cardboard sheet covering the chambers was

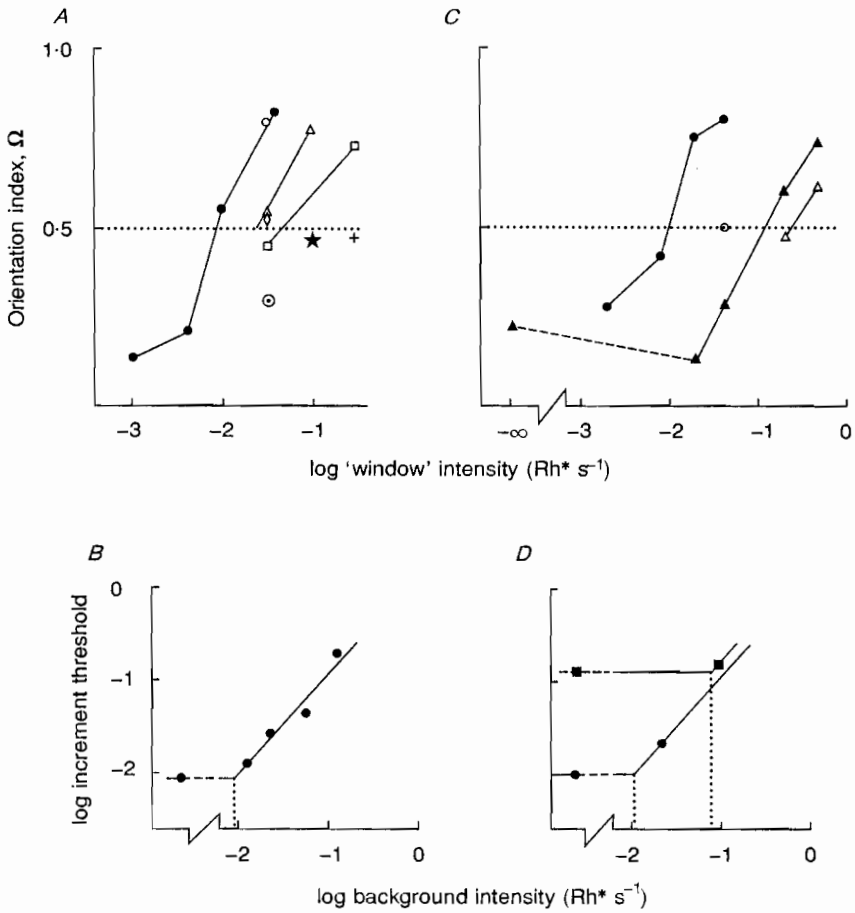


Fig. 4. Deterioration of jumping orientation with increasing intensity of light surrounding the lit window ('background'). Panels *A* and *C* show original orientation data, while panels *B* and *D* show increment-threshold functions extracted from these data. *A*, *R. temporaria*, 15–16 °C. Abscissa, log window intensity ( $\text{Rh}^* \text{s}^{-1}$ ); ordinate, orientation index. ●, data in darkness, reproduced from Fig. 2. Other symbol types refer to a set of sessions at one intensity of the surrounding background ( $\text{Rh}^* \text{s}^{-1}$ ): 0.004 (○), 0.013 (△), 0.019 (◇), 0.023 (□), 0.030 (⊙), 0.059 (★) and 0.133 (+). The *increment* threshold against a certain background is obtained as threshold window intensity minus background intensity. *B*, increment-threshold function derived from the data in *A*. Ordinate, log increment threshold; abscissa, log background intensity. The vertical dotted line marks the dark light, 0.009  $\text{Rh}^* \text{s}^{-1}$ . *C*, jumping orientation in *R. pipiens* (displayed as in *A*) at two temperatures: 16–17 °C (circles) and 23–24 °C (triangles). Filled symbols, data in darkness; open symbols, data obtained with background intensities 0.023  $\text{Rh}^* \text{s}^{-1}$  (◇) and 0.094  $\text{Rh}^* \text{s}^{-1}$  (△). *D*, dark lights at 16–17 and 23–24 °C (vertical dotted lines) derived from the data in *C* by the same conventions as in *B*.

replaced by gelatin filter sheets of desired optical density with circular windows in the same positions as in the cardboard (see Methods). The lit window then appears as a brighter area in a dimly lit surround, with contrast depending on the density

of the filter sheet. The intensity of the surround represents 'background' intensity. 'Stimulus' intensity is window minus background.

Figure 4A and B illustrates the construction of a frog increment-threshold function at one temperature (15–16 °C). Panel A plots orientation indices as a function of window intensity. The orientation function recorded in darkness (the same as shown in Fig. 2A) is marked by filled circles. Each of the other symbol types represents data obtained at one background intensity. To make the dark light values comparable with retinal values derived further below from ganglion cell recordings in the opened eye, light intensities are given not as corneal illumination, but as rates of photoisomerizations in rods (see Methods).

First consider the vertical column of data points at a single *window* intensity (log intensity  $-1.5$ , or  $0.033 \text{ Rh}^* \text{ s}^{-1}$ ). These are well ordered according to background intensity, the highest point ( $\odot$ ) recorded at the lowest and the lowest point ( $\ominus$ ) recorded at the highest background intensity. In other words, orientation deteriorated monotonically with increasing background. Note, however, that stimulus-background contrast also decreases from top to bottom (since window intensity is constant).

Pairs of points recorded at the same *background* intensity are connected with straight lines, forming a segment of the orientation function against that background (shown in Fig. 4A for backgrounds  $0.013$  and  $0.023 \text{ Rh}^* \text{ s}^{-1}$ ). The effect of background illumination is mainly to shift the function to the right (towards higher window intensities). Then, to a first approximation, even single data points suffice to define the shift due to a background. The symbols  $\star$  and  $+$  (which lie practically on the  $\Omega = 0.5$  line) define thresholds to two stronger backgrounds ( $0.059$  and  $0.133 \text{ Rh}^* \text{ s}^{-1}$ ).

Figure 4B is a conventional log-log plot of increment threshold (i.e. window threshold minus the respective background intensity in Fig. 4A) against background intensity. The slope of the regression line is  $1.1$ . Thus, for large targets of long duration, the frog's background adaptation approximates Weber's law. It should be noted that this is not due to photoreceptor adaptation: even the strongest background intensity ( $0.133 \text{ Rh}^* \text{ s}^{-1}$ ) used here is about three times weaker than that where anuran rods start to desensitize (Hemilä, 1977; Donner, Copenhagen & Reuter, 1990a). The illumination-equivalent dark light is obtained as the background intensity where the sloping and horizontal parts intersect, at  $0.009 \text{ Rh}^* \text{ s}^{-1}$ .

Figure 4C and D presents results of experiments to determine the dark light at two different temperatures (16–17 and 23–24 °C) in one batch of *R. pipiens*. Thresholds in darkness and against one background intensity were determined at both temperatures. Figure 4D shows how the dark lights were estimated by extrapolating a line of slope  $1.1$  (see above) from the 'background' threshold point down to the horizontal line marking the dark-adapted threshold level. The values obtained are  $0.011$  and  $0.080 \text{ Rh}^* \text{ s}^{-1}$ , respectively. As the temperature difference was  $7$  °C, this increase corresponds to  $Q_{10} = 17$ .

#### Retinal ganglion cell thresholds

To distinguish retinal and possible central components of the temperature effect on visual sensitivity, spiking thresholds of retinal ganglion cells were recorded at

two or three temperatures between 9 and 22 °C. Winter *R. temporaria* from the same population as in the behavioural study were used. We started at the lowest temperature, warmed and then returned to repeat the measurements at the low temperature. Reasonably complete results were obtained from thirteen cells.

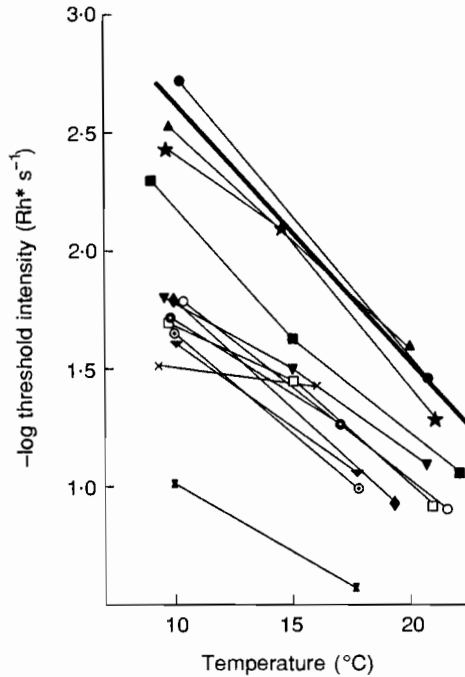


Fig. 5. Sensitivities of thirteen dark-adapted ganglion cells from the retina of *R. temporaria* to large-field step stimuli as functions of temperature. Ordinate, log sensitivity (reciprocal of the threshold intensity expressed in  $\text{Rh}^* \text{s}^{-1}$ ). Abscissa, temperature ( $^{\circ}\text{C}$ ). Each symbol type refers to one cell. The low-temperature point for each cell gives the mean of sensitivities recorded before and after recordings at high temperature, except for three cells where a second low-temperature sensitivity measurement was not obtained (the cells marked by  $\blacktriangle$  and  $\blacktriangledown$  and  $\bullet$ ). The bold line of slope  $-1.09$  per  $10^{\circ}\text{C}$  is the regression line for those jumping thresholds (in Fig. 3) that lie within the same temperature interval as the ganglion cell data ( $\leq 22^{\circ}\text{C}$ ). The units of Fig. 3 ( $525 \text{ nm quanta mm}^{-2} \text{ s}^{-1}$ ) have been converted into  $\text{Rh}^* \text{s}^{-1}$  by multiplying by the factor  $10^{-4}$  (*R. temporaria*: entrance pupil  $10 \text{ mm}^2$ , 91 % transmission, 32 % of 525 nm quanta isomerize, and the retinal image of the window covers 29 200 rods;  $(10 \times 0.91 \times 0.32)/29\,200 = 10^{-4}$ . *R. pipiens*: entrance pupil  $10.2 \text{ mm}^2$ , 91 % transmission, 40 % of 525 nm quanta isomerize, and the retinal image of the window covers 36 400 rods;  $(10.2 \times 0.91 \times 0.40)/36\,400 = 10^{-4}$ . See Methods for details.)

The log sensitivities ( $1/\text{threshold}$ ) of these cells in detecting a stimulus equivalent to the lit window of the behavioural experiments are plotted in Fig. 5 as functions of temperature. Three of the cells (see figure legend) were lost before a reliable second threshold determination was obtained at low temperature (after returning from high temperature). In the remaining ten cells, the second low-temperature

threshold was on average 0.16 log units (45%) higher than the original one. For these cells the low-temperature values shown in Fig. 5 are means of two (or, in some cells, three) measurements.

In all cells, log sensitivity fell steeply and near-linearly with increasing temperature. The mean slope is  $-0.75 \pm 0.07$  log units per  $10^\circ\text{C}$ . It is most appropriate to compare this with the decrease in behavioural sensitivity over the *same temperature interval* (bold line of slope  $-1.09$  log units per  $10^\circ\text{C}$  in Fig. 5, based on the data for temperatures below  $22^\circ\text{C}$  in Fig. 3). It is somewhat shallower than for the full temperature range covered in the jumping experiments, but still significantly steeper than the average ganglion cell slope. However, absolute sensitivity in this sample of ganglion cells varied 50-fold at  $10^\circ\text{C}$ , and only four were within 0.5 log units of the sensitivity expressed in behaviour. The sensitivities of these four cells followed a mean slope of  $-1.0 \pm 0.06$  log units per  $10^\circ\text{C}$ . In view of the systematic tendency for higher sensitivity to be associated with steeper temperature dependence, we think that the larger value is more representative of cells active at the absolute behavioural threshold. It is not significantly different from the slope describing the behavioural data. We therefore conclude that the dominant mechanisms underlying the temperature dependence of behavioural sensitivity reside in the retina. This also means that the phenomenon can be quantitatively analysed at the level of the retinal ganglion cell.

#### *Summation times and threshold numbers of isomerizations*

Changes in the threshold to a stimulus of large spatial extent and long duration could depend on changes in either the threshold number of isomerizations  $M_t$  or the summation parameters  $A_s$  or  $t_t$  (eqn (2)). In six of the cells included in Fig. 5,  $A_s$  (receptive field size) was determined at both low and high temperature. (Among these were the two most sensitive cells.) The mean change when going from 10 to  $20^\circ\text{C}$  amounted to  $-3 \pm 10\%$ . We concluded that  $A_s$  is not significantly affected by temperature and chose to compress the experimental protocol in other cells by omitting determination of  $A_s$  at high temperature, thus improving the prospects for completing more urgent measurements.

#### *Summation times*

Changes in both  $t_t$  and  $M_t$  contributed to the changes in 'step' sensitivity, and Fig. 6 resolves the two factors. The plots are similar to Fig. 5, with logarithmic ordinates against a linear temperature abscissa. First consider summation times (Fig. 6A). Log  $t_t$  shows a roughly linear relation to temperature, with comparatively minor differences between sensitive and less sensitive cells. The mean slope is  $-0.38 \pm 0.04$  log units per  $10^\circ\text{C}$ , which corresponds to  $Q_{10} = 2.4$ .  $Q_{10}$  values reported for the time to peak of dim-flash rod responses are 2.1 in *R. temporaria* (Donner *et al.* 1988; mass receptor potential from isolated retina) and 2.2 in *Bufo marinus* (Lamb, 1984; photocurrent from isolated rods). Assuming that the shape of rod responses remains invariant under temperature changes, integration time is directly proportional to the time to peak of the dim-flash response. Then the

decrease in ganglion cell summation times is mainly attributable to acceleration of rod responses (shown as a dotted line in Fig. 6A).

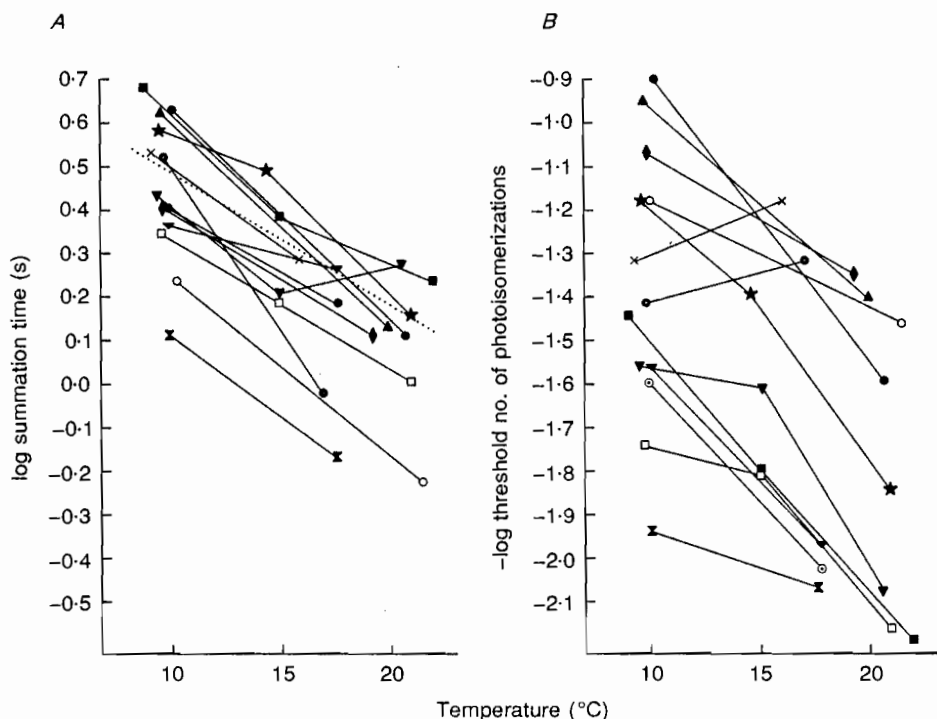


Fig. 6. *A*, log summation times (s) and *B*, log flash sensitivity (reciprocal of threshold numbers of photoisomerizations within  $A_s$  and  $t_1$ ) of the same sample of ganglion cells as in Fig. 5, as functions of temperature (abscissa). The dotted line in *A* shows how the integration time of rod responses from *R. temporaria* shortens with rising temperature (Donner *et al.* 1988).

#### Flash thresholds

The rest of the change in step thresholds is due to a change in the threshold number of photoisomerizations  $M_t$  (plotted in Fig. 6*B* as log sensitivity,  $\log(1/M_t)$ ). If the temperature dependence is again expressed as the slope of a straight line relating  $\log(1/M_t)$  to temperature, the mean slope in our sample of ganglion cells is  $-0.37$  per  $10^\circ\text{C}$  (trivially,  $= -(0.75 - 0.38)$ ). However,  $\log(1/M_t)$  in the four cells that were most sensitive when studied with large, long stimuli (see Fig. 5) had a significantly steeper temperature dependence, with a mean slope of  $-0.56 \pm 0.08$  between 10 and  $20^\circ\text{C}$  ( $Q_{10} = 3.6$ ).

#### Changes in intrinsic variability measured from ganglion cell threshold performance

Retinal noise affects the statistics of ganglion cell responses to light flashes of near-threshold intensities. The magnitude of the noise underlying ganglion cell

performance can therefore be estimated from the shape of the frequency-of-response functions; stronger noise gives shallower curves. In four cells we obtained noise estimates at both low and high temperature by this method. The noise was quantified by translating it into equivalent quantal fluctuations from a dark light (see Methods).

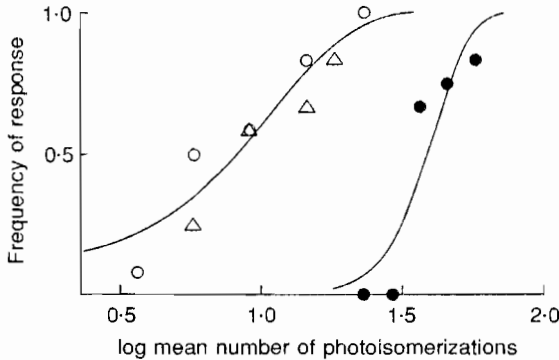


Fig. 7. Frequency-of-response functions recorded with flash stimuli at two temperatures from the most sensitive ganglion cell (the cell marked by ● in Figs 5 and 6). Every data point gives the fraction of responses out of twelve trials with a flash of the same mean intensity (abscissa, log mean number of photoisomerizations from the flash). Different flash intensities were presented in pseudo-random order. The open symbols refer to data recorded at 10.2 °C before (○) and after (△) the period at 20.7 °C (●). The smooth curves are the best-fitting cumulative Poisson functions, with parameters ( $M_v$ ,  $X$ ) = (8, 40) and (39, 105), respectively.

Figure 7 shows the results of a frequency-of-response experiment on our most sensitive ganglion cell (● in Figs 5 and 6). Data were recorded first at 10.2 °C (○), then at 20.7 °C (●) and then again at 10.2 °C (△). The curves are maximum-likelihood fits of cumulative Poisson functions (eqn (4)). As described in the Methods, this provides estimates of mean numbers of photon-like events ( $X$ ) pooled with the flashes (i.e. occurring within  $A_s$  and  $t_f$ ) that would explain the variability not accounted for by variation in the photon content of flashes. In this cell, the best fit was obtained with  $X = 40$  at 10.2 °C and  $X = 105$  at 20.7 °C. Owing to shorter  $t_f$  at the higher temperature, the resulting dark light estimates ( $I_x = X/Rt_f$ , eqn (5)) differ more strongly: 0.011 vs. 0.092  $\text{Rh}^* \text{s}^{-1}$ . The mean values at 10 and 20 °C in four cells were  $0.009 \pm 0.002$  and  $0.10 \pm 0.02 \text{ Rh}^* \text{s}^{-1}$ , respectively. This indicates an 11-fold increase in the noise-equivalent dark light per 10 °C temperature rise.

The noise standard deviation due to a mean event number  $X$  is proportional to  $\sqrt{X}$ . In the cell in Fig. 7, noise summed with the flash thus grew by a factor of  $\sqrt{(105/40)} = 1.6$  between 10 and 20 °C. A simple noise-limitation hypothesis states that the flash threshold should rise by the same factor (de Vries, 1943; Rose, 1948), but the threshold rise in this cell was almost 5-fold. In the four cells where noise was estimated by frequency-of-response functions, mean noise increased by a factor of  $2.0 \pm 0.2$ , while mean flash threshold rose by a factor of  $3.4 \pm 0.7$ . Thus, the sensitivity decrease was clearly greater than the noise increase.



This conclusion is borne out by changes in the maintained discharges of cells. In healthy amphibian ganglion cells, the rate of spontaneous spiking can often be explained as the probability that excursions of retinal noise alone (without any light) exceed the ganglion cell spike threshold (eqn (7) in Aho *et al.* 1987). If so, a

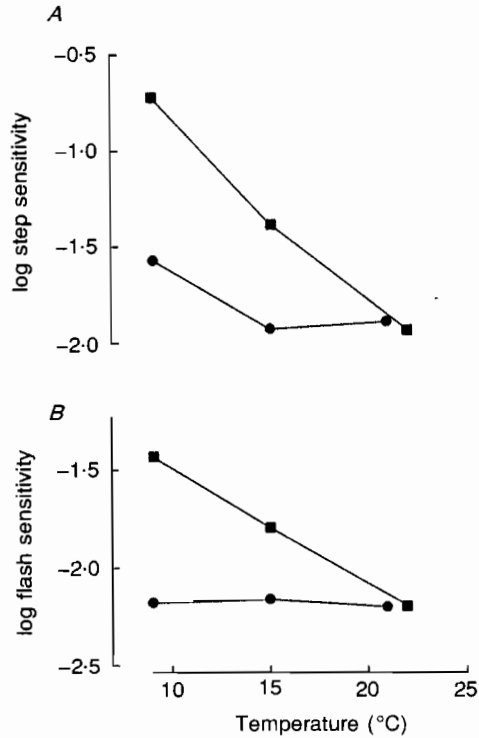


Fig. 8. Weakening of the temperature dependence of ganglion cell sensitivity under a steady background light of intensity  $0.3 \text{ Rh}^* \text{ s}^{-1}$  (from the cell marked by ■ in Figs 5 and 6). *A*, step thresholds; *B*, flash thresholds. ■, in darkness (same data as in Figs 5 and 6); ●, under background light. Abscissa, temperature ( $^{\circ}\text{C}$ ). Ordinate in *A*, log step sensitivity, reciprocal of the threshold rate of photoisomerizations within the receptive field ( $\text{s}^{-1}$ ); ordinate in *B*, log flash sensitivity, reciprocal of the threshold number of photoisomerizations within the receptive field.

desensitization larger than the average noise increase must be evident as a reduced rate of maintained discharge. Indeed, in all the 'behaviour-like' cells, the rate of maintained discharge fell significantly at higher temperatures. For example, a calculation from the flash sensitivities and noise estimates for the cell in Fig. 7 predicts a maintained discharge rate of  $4.3 \text{ spikes min}^{-1}$  at  $10.2^{\circ}\text{C}$  falling to less than 1 spike per 200 min at  $20.7^{\circ}\text{C}$ . The observed rates in this cell were  $6 \text{ min}^{-1}$  at  $10.2^{\circ}\text{C}$ , falling to zero over a 10 min sampling interval at  $20.7^{\circ}\text{C}$ , in fair agreement with the theory.

*The temperature dependence can be decreased by background light*

The degree to which noise is involved in the thermal elevation of ganglion cell flash thresholds was further studied by the following logic. If sensitivity is limited by additive intrinsic noise which increases with temperature, the temperature effect should disappear when strong enough extrinsic noise is added. This was done by applying background lights (i.e. known amounts of quantal noise). The results from one cell are shown in Fig. 8 (the cell marked by filled squares in Figs 5 and 6).

The background of intensity  $0.3 \text{ Rh}^* \text{ s}^{-1}$  abolished the temperature dependence of  $M_t$ . In the step thresholds, a weak dependence remained, indicating that summation times still shortened moderately with warming. The results obtained from similar experiments in two other cells were consistent, although the temperature dependence of  $M_t$  was not completely abolished.

#### DISCUSSION

*The temperature effect on visual sensitivity*

The temperature effect on absolute visual sensitivity is strong and regular. On average, warming by  $10^\circ \text{C}$  brought a  $1.26$  log unit sensitivity decrease for the task of detecting a lit window, i.e. a target extended in space and permanent in time. The relation was basically similar for *R. temporaria* and *R. pipiens*, and no difference was found between winter and summer frogs. Muntz & Northmore (1968) have previously reported that the increment threshold of turtles against a very weak background rose by a factor of five when temperature was raised from  $20$  to  $30^\circ \text{C}$ . Quantitative comparisons with our results are difficult as absolute sensitivities in terms of isomerization rates in rods cannot be reliably calculated from their published data.

*Retinal origin of the effect*

The absolute visual threshold of freely behaving *R. temporaria* corresponded to  $0.004 \text{ Rh}^* \text{ s}^{-1}$  at the temperature  $11.5^\circ \text{C}$ . At this temperature, we have previously collected a large amount of material on absolute thresholds of ganglion cells sampled by our microelectrodes. Of the 105 cells considered by Donner (1989), seven cells were sensitive enough to 'see' a  $0.004 \text{ Rh}^* \text{ s}^{-1}$  stimulus on at least half of the trials; here we had one cell out of thirteen. Of those sampled, the percentage of sufficiently sensitive cells was thus  $100 \times (8/118) \approx 7\%$ . Possibly, our microelectrodes pick up only 'large' cells (Kalinina, 1976; Kock, Mecke, Orlov, Reuter, Väisänen & Wallgren, 1989), so it must be allowed that cells active at the behavioural threshold may constitute no more than  $0.1\text{--}1\%$  of all ganglion cells in the frog retina. With their large receptive fields (mean  $A_s$  in the 8 sufficiently sensitive cells was  $0.063 \text{ mm}^2$ ) they are still likely to provide complete coverage of the visual field (Donner, 1989). The high statistical significance of spike responses in frog ganglion cells makes it understandable that behaviour can in principle rely on a small number of sensitive cells.

The present results show that behavioural sensitivity parallels that of the most sensitive ganglion cells even over the more than 10-fold sensitivity change from 10 to 20 °C. Thus, the temperature effect on behaviourally measured sensitivity contains no substantial components of other than retinal origin.

*Is the temperature dependence of ganglion cell flash sensitivity due to thermal noise?  
Excessive desensitization*

Of the 10-fold sensitivity drop between 10 and 20 °C in the four most 'behaviour-like' ganglion cells, a factor of 2.9 was due to decreased temporal summation and a factor of 3.6 to decreased flash sensitivity. Most of the former change can be accounted for by acceleration of rod responses (see Fig. 6A). The frequency-of-response experiments, however, clearly showed that the drop in ganglion cell flash sensitivity (rise in flash thresholds) was excessive from the viewpoint of maintaining a constant signal-noise ratio for threshold responses (de Vries, 1943; Rose, 1948). Stated somewhat differently: the temperature effect is not due to a mechanism whereby ganglion cells are desensitized exactly in proportion to the standard deviation of noise summed over  $A_s$  and  $t_1$  ('noise adaptation'; Donner *et al.* 1990 a).

*Arguments for noise limitation*

Given this quantitative discrepancy, what grounds are there to assume a *causal* relation between the retinal noise and the rise in ganglion cell thresholds? The main argument is that the temperature dependence of flash thresholds could be abolished by a dim background light, supposedly clamping noise at the level set by photon fluctuations (Fig. 8). Similarly, Muntz & Northmore (1968) found that turtle increment thresholds depended on temperature only at the lowest background intensity they used. This disappearance of thermal desensitization is not a consequence of the 'predesensitization' by the adapting background, because the thresholds of ganglion cells where sensitivity has been even more strongly depressed by *bleaching* exposures have been shown to display a high degree of temperature dependence during the course of dark-adaptation (Donner & Reuter, 1967). From our present viewpoint, we think the latter observation in fact supports the idea that elevated rod noise may cause part of the loss of visual sensitivity persisting for tens of minutes after pigment bleaches (Barlow, 1964; Lamb, 1980, 1981).

*The size of rod photoresponses*

An alternative possibility that merits comment is that the amplitude of rod photoresponses could decrease so as to limit ganglion cell sensitivity at higher temperatures. However, in our *R. temporaria*, dim-flash current responses of rods grow with rising temperature up to ca 17 °C and decrease significantly only above 20 °C (mass receptor recordings by Donner *et al.* (1988); cf. also current recordings from single rods of *Bufo marinus* by Baylor *et al.* (1983) and Lamb (1984)). Admittedly, the light-sensitive current of the rods grows monotonically with temperature over the whole interval, so *relative* sensitivity (the percentage of the light-sensitive current turned off by a photon absorption) stays practically constant between 10 and 17 °C, and starts falling rather steeply from about 18 °C. Still, the

evidence from electroretinogram and current recordings suggests that reduction of rod response amplitude could contribute to the thermal desensitization only in the upper end of the temperature range covered in our experiments. On the other hand, the temperature dependence of rod voltage responses (the functionally relevant signal) or e.g. the gain of the rod-bipolar synapse are not known.

*Is the dark light due to thermal isomerizations in rods?*

Noise has here been quantified by translating it into an equivalent dark light, with units of isomerizations per rod per second. As such, this is no more than a formal description, but it will inevitably suggest that the source is really thermal isomerizations in rods (Barlow, 1956; Baylor *et al.* 1980; Copenhagen *et al.* 1987; Donner, 1989). Our present results would seem to conflict with this idea. The rate of spontaneous discrete events in toad rods measured by Baylor *et al.* (1980) increased with a  $Q_{10}$  of only 3.8 between 10 and 20 °C, corresponding to an apparent activation energy  $E_a$  of 21.9 kcal mol<sup>-1</sup>. This is significantly less than estimated here for frog dark light. The illumination-equivalent dark light measured in behavioural experiments increased with  $Q_{10} = 17$ , corresponding to  $E_a = 47$  kcal mol<sup>-1</sup>. The noise-equivalent dark light estimated from ganglion cell frequency-of-response functions increased with  $Q_{10} = 11$ , suggesting  $E_a = 39$  kcal mol<sup>-1</sup>.

A similar discrepancy has been evident for more than 10 years between the thermal parameters of Baylor *et al.* (1980) and those derived by Ashmore & Falk (1977) from membrane voltage fluctuations in dogfish bipolar cells. The latter authors found an apparent activation energy of 36 kcal mol<sup>-1</sup> (giving  $Q_{10} = 9.0$  between 10 and 20 °C) for rod events that would account for the noise they recorded. In principle, bipolar cells might of course be affected by noise of post-transduction origin. However, an alternative, equally reasonable interpretation is that the parameters of Baylor and colleagues, although based on direct recordings from single rods, are not universally valid. Firstly, the seemingly fundamental agreement between the thermal parameters of their rod event rates and those for isomerization of 11-*cis*-retinal in digitonin solution (Hubbard, 1966) is weakened by the fact that the absolute rates in solution were higher by three orders of magnitude. Secondly, in rhodopsin rods of *Rana catesbeiana*, whose rhodopsin is spectrally similar to that of *Bufo marinus*, much lower absolute rates of isomerization-like dark events have been recorded (Donner, Firsov & Govardovskii, 1990 *b*). Thermal isomerization of visual pigment may be sensitive not only to opsin structure, but also to the environment of the molecule. We therefore think it would be premature to exclude spontaneous isomerization of rhodopsin as a major source of thermal dark light.

This work was supported by the Academy of Finland (01/455 and 01/1011872). We thank Mr Åke Vuorisalo for making the photographs of dark-adapted frogs from which pupil sizes were measured.

#### REFERENCES

- AGUILAR, M. & STILES, W. S. (1954). Saturation of the rod mechanism of the retina at high levels of stimulation. *Optica Acta* **1**, 59-65.
- AHO, A.-C., DONNER, K., HYDÉN, C., LARSEN, L. O. & REUTER, T. (1988). Low retinal noise in animals with low body temperature allows high visual sensitivity. *Nature* **334**, 348-350.

- AHO, A.-C., DONNER, K., HYDÉN, C., REUTER, T. & ORLOV, O. YU. (1987). Retinal noise, the performance of retinal ganglion cells, and visual sensitivity in the dark-adapted frog. *Journal of the Optical Society of America A* **4**, 2321–2329.
- ASHMORE, J. F. & FALK, G. (1977). Dark noise in retinal bipolar cells and stability of rhodopsin in rods. *Nature* **270**, 69–71.
- BARLOW, H. B. (1956). Retinal noise and absolute threshold. *Journal of the Optical Society of America* **46**, 634–639.
- BARLOW, H. B. (1957). Increment thresholds at low intensities considered as signal/noise discriminations. *Journal of Physiology* **136**, 469–488.
- BARLOW, H. B. (1964). Dark-adaptation: a new hypothesis. *Vision Research* **4**, 47–58.
- BARLOW, H. B. (1977). Retinal and central factors in human vision limited by noise. In *Vertebrate Photoreception*, ed. BARLOW, H. B. & FATT, P., pp. 337–358. Academic Press, London.
- BAYLOR, D. A., MATTHEWS, G. & YAU, K.-W. (1980). Two components of electrical dark noise in toad rod outer segments. *Journal of Physiology* **309**, 591–621.
- BAYLOR, D. A., MATTHEWS, G. & YAU, K.-W. (1983). Temperature effects on the membrane current of the toad. *Journal of Physiology* **337**, 723–734.
- COPENHAGEN, D. R., DONNER, K. & REUTER, T. (1987). Ganglion cell performance at absolute threshold in toad retina: effects of dark events in rods. *Journal of Physiology* **393**, 667–680.
- DE VRIES, H. (1943). The quantum character of light and its bearing upon the threshold of vision, the differential sensitivity and visual acuity of the eye. *Physica* **10**, 553–564.
- DONNER, K. (1987). Adaptation-related changes in the spatial and temporal summation of frog retinal ganglion cells. *Acta Physiologica Scandinavica* **131**, 479–487.
- DONNER, K. (1989). The absolute sensitivity of vision: can a frog become a perfect detector of light-induced and dark rod events? *Physica Scripta* **39**, 133–140.
- DONNER, K. (1992). Noise and the absolute thresholds of cone and rod vision. *Vision Research* **32**, 853–866.
- DONNER, K., COPENHAGEN, D. R. & REUTER, T. (1990 *a*). Weber and noise adaptation in the retina of the toad *Bufo marinus*. *Journal of General Physiology* **95**, 733–753.
- DONNER, K., FIRSOV, M. L. & GOVARDOVSKII, V. I. (1990 *b*). The frequency of isomerization-like 'dark' events in rhodopsin and porphyropsin of the bull-frog retina. *Journal of Physiology* **428**, 673–692.
- DONNER, K., HEMILÄ, S. & KOSKELAINEN, A. (1988). Temperature-dependence of rod photoresponses from the aspartate-treated retina of the frog (*Rana temporaria*). *Acta Physiologica Scandinavica* **134**, 535–541.
- DONNER, K. O. & REUTER, T. (1967). Dark-adaptation processes in the rhodopsin rods of the frog's retina. *Vision Research* **7**, 17–41.
- DU PONT, J. S. & DE GROOT, P. J. (1974). A schematic dioptric apparatus for the frog's eye (*Rana esculenta*). *Vision Research* **16**, 803–810.
- FECHNER, G. T. (1860). *Elemente der Psychophysik*. Breitkopf & Härtel, Leipzig.
- GOVARDOVSKII, V. I. & ZUEVA, L. V. (1974). Spectral sensitivity of the frog eye in the ultraviolet and visible region. *Vision Research* **14**, 1317–1321.
- HARRI, M. E. (1973). The rate of metabolic temperature acclimation in the frog, *Rana temporaria*. *Physiological Zoology* **46**, 148–156.
- HEMILÄ, S. (1977). Background adaptation in the rods of the frog's retina. *Journal of Physiology* **265**, 721–741.
- HEMILÄ, S. & REUTER, T. (1981). Longitudinal spread of adaptation in the rods of the frog's retina. *Journal of Physiology* **310**, 501–528.
- HUBBARD, R. (1966). The stereoisomerism of 11-cis retinal. *Journal of Biological Chemistry* **241**, 1814–1818.
- KALININA, A. V. (1976). Quantity and topography of frog's retinal ganglion cells. *Vision Research* **16**, 929–934.
- KOCK, J.-H., MECKE, E., ORLOV, O. YU., REUTER, T., VÄISÄNEN, R. A. & WALLGREN, J. E. C. (1989). Ganglion cells in the frog retina: discriminant analysis of histological classes. *Vision Research* **29**, 1–18.
- LAMB, T. D. (1980). Spontaneous quantal events induced in toad rods by pigment bleaching. *Nature* **287**, 349–351.

- LAMB, T. D. (1981). The involvement of rod photoreceptors in dark adaptation. *Vision Research* **21**, 1773-1782.
- LAMB, T. D. (1984). Effects of temperature changes on toad rod photocurrents. *Journal of Physiology* **346**, 557-578.
- LIEBMAN, P. A. & ENTINE, G. (1968). Visual pigments of frog and tadpole (*Rana pipiens*). *Vision Research* **8**, 761-775.
- MATTHEWS, R. G., HUBBARD, R., BROWN, P. K. & WALD, G. (1963). Tautomeric forms of metarhodopsin. *Journal of General Physiology* **47**, 215-240.
- MUNTZ, W. R. A. (1962). Effectiveness of different colors of light in releasing the positive phototactic behavior of frogs, and a possible function of the retinal projection to the diencephalon. *Journal of Neurophysiology* **25**, 712-720.
- MUNTZ, W. R. A. & NORTHMORE, D. P. M. (1968). Background light, temperature and visual noise in the turtle. *Vision Research* **8**, 787-800.
- PUTNAM, R. W. & BENNETT, A. F. (1981). Thermal dependence of behavioural performance of anuran amphibians. *Animal Behaviour* **29**, 502-509.
- REUTER, T., DONNER, K. & COPENHAGEN, D. R. (1986). Does the random distribution of discrete photoreceptor events limit the sensitivity of the retina? *Neuroscience Research*, suppl. **4**, S163-180.
- ROSE, A. (1948). The sensitivity performance of the human eye on an absolute scale. *Journal of the Optical Society of America* **38**, 196-208.